Hindawi
International Journal of Aerospace Engineering
Volume 2019, Article ID 5987306, 15 pages
https://doi.org/10.1155/2019/5987306

Research Article

Modular Motion-Structure Design Model for Planetary Surface Sampling

Qian Li,[1] **Lanlan Xie**,[1,2] **and Junping Li**[3,4]

[1]*College of Environment and Civil Engineering, Chengdu University of Technology, Chengdu 610059, China*
[2]*State Key Laboratory of Geohazard Prevention and Geoenvironment Protection, Chengdu University of Technology, Chengdu 610059, China*
[3]*Institute of Exploration Technology, CAGS, Chengdu 611734, China*
[4]*Technical Center for Geological Hazard Prevention and Control, CGS, Chengdu 611734, China*

Correspondence should be addressed to Qian Li; liqian2014@cdut.edu.cn

Received 16 October 2018; Accepted 15 January 2019; Published 1 April 2019

Academic Editor: Joseph Morlier

Because there are less restrictions in space, a variety of different movement patterns and equipment structures may be used during the process of planetary surface sampling. Traditionally, the optimal analysis for surface sampling is focused on specific equipment structures and movements; in contrast, a new modular motion-structure design model for surface sampling, which is a more flexible model, is discussed in this paper. By establishing and combining two basic module groups, namely, the motion group and the structure group, this new design model can define and analyse multiple movement patterns and structures. For the motion group, calculating the sampling trajectory is the main purpose, in which there are two basic modules: tridimensional uniform rectilinear movements and tridimensional uniform circular movements. The two basic motion modules can be freely combined in a given coordinate system to simulate a random sampling trajectory. The structure group contains a series of curved and flat plates, which can be defined by a set of unified parameters (including section, extension, and cutting parameters). By assigning different values to these parameters, the curved or flat plates can represent different external shapes. The different structures of the various pieces of surface sampling equipment can be simulated by combining these different plates. In addition to defining these basic modules, analysing the coupling among different modules, which can be simplified to the relationship between velocity and surface, plays an important role in establishing this design model. Based on the modular design theory, this new model will not only reduce the difficulty of analysis but also improve accuracy for planetary surface sampling.

1. Introduction

Research on extraterrestrial planets will be ongoing because of the ability of human beings to explore the universe. In the scientific field, this type of research can enrich the theories of the planets, the environment, the origin of life, and other related areas. Research on extraterrestrial planets can also bring significant developments in the areas of science, economy, military, etc. Since the Chinese lunar exploration project started in 2004, named Chang'e, the target of exploring the Moon in the first stage has been completed, and the second stage is focused on a lunar soft landing; an automatic inspection survey is now in progress. According to the research plan, the third stage of landing on the Moon, the sampling of lunar soil and return to Earth, will be completed sometime between 2017 and 2020 [1]. Meanwhile, the Chinese exploration of Mars will begin approximately in 2020, and this mission is expected to launch an exploratory rover to complete some preliminary investigations.

To study extraterrestrial planets, sampling is the most direct and effective method; however, it is also a difficult method to implement. Planetary sampling methods are widely studied by many countries around the world. According to the difference of sampling depth, the planetary sampling can be divided into surface sampling and deep sampling, and the two sampling modes also require different

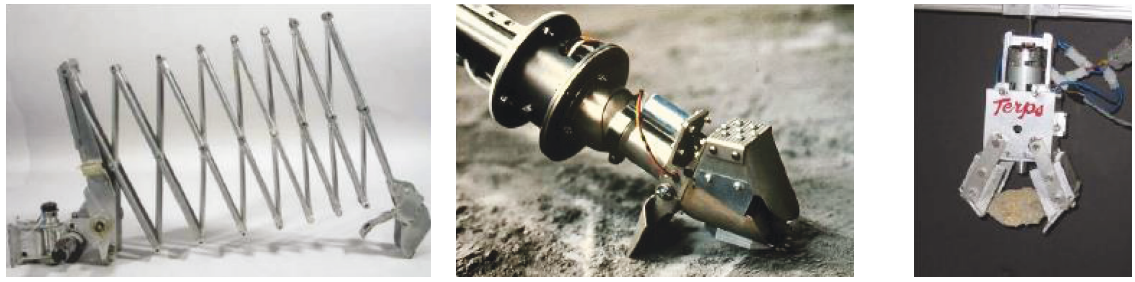

(a) (b) (c)

Figure 1: Various surface sampling equipment structures: (a) digging, (b) shovelling, and (c) clamping.

sampling movements and equipment structures. For deep sampling, drilling is nearly the only way to obtain samples because of the limited movement space. For example, drilling was used in the lunar projects of Luna (Russia) and Apollo (U.S.A.), the Venusian project of Venera (Russia), the Martian projects of Deep Space 2 (U.S.A.) and Beagle 2 (EU), the cometary project of Rosetta (EU), etc. [2]. And in recent researches, some of the researchers also start to develop relative new sampling mode similar to drilling in order to increase sampling efficiency; for instance, the dual-reciprocating drill system developed by the University of Surrey can control the lateral movements and increase drilling depth [3, 4]. Compared with deep sampling, because there is hardly any space limitations, the sampling movement and equipment structure of surface sampling are more complex. According to the actual surface sampling projects for Moon, Mars, and Venus, a variety of sampling devices have been used to perform many tasks, such as digging, shovelling, clamping, grinding (to obtain the rock powder through grinding), and adsoring (to obtain dust through electrostatic adsorption), as shown in Figure 1 [2, 5–8]. Even for the same sampling movement, different equipment structures may be used; e.g., NASA had developed three different types of digging structures [8].

In the area of sampling devices research, there are two typical directions, one of the directions is focused on the entire systems which are considered as a robot. In this direction, the robots are usually researched by using the explicit mention of Lagrangian formalisms adapted to robotics. For instance, on the basis of the Kane equation that developed to describe the dynamic behavior for constrained multi-degree-of-freedom discrete system, the dynamic modelling and control method for a bicycle robot and hydraulic excavator have been developed by Beijing University of Posts and Telecommunications and University of Kragujevac, respectively [9, 10]. And according to research, Texas A&M University proposed analytical dynamics of variable-mass systems through the theory similar to the Lagrange equation, Appell equations, and Kane equations [11]. This direction pays much more attention on the entire system and therefore can hardly figure out the reaction force acting on the sampling devices.

On the other hand, when the researches are focused on the sampling devices, either abroad or domestic, they are typically focused on the areas of specific movement and equipment structure. For instance, Carnegie Mellon University developed continuous excavation device, Jinlin University measured the torque using a specific scoop during sampling, and the University of California at Berkeley carried out several experiments for percussive excavation at different atmospheric pressures with a specially designed scoop [12–14]. This research approach limits the analysis accuracy and application. The various movements and structures increase the difficulty of theoretical analysis and design optimization in this area.

To avoid the mentioned problems, a more flexible modular motion-structure design model for planetary surface sampling is discussed in this paper. This design model consists of two module groups, the motion and structure groups, and each group is composed of several basic modules (Figure 2(b)). The basic modules from the same group should have the same parameter structure (Figure 2(a)). By combining these different basic modules, the new design model can be applied to design or analyse different movements and equipment structures (Figure 2(c)); as a result, this model is appropriate for the characteristics needed for planetary surface sampling.

2. Motion Module Group

2.1. Motion Module Definition. The main function of the motion module group is to define the different motion patterns and draw a sampling trajectory for the surface sampling process. Based on the modular design concept, each basic module should be a separate part that has standard input and output parameters and an independent function. Hence, the sampling motion should be independent from the equipment structure, and the sampling equipment will be simplified to a particle P in the motion module group definition. The first step is to establish a coordinate system: a tridimensional coordinate system XYZ is built on the planetary surface, and the planetary ground plane is assumed to be plane XOY. Next, the motion modules are defined as mathematical models used to calculate the current coordinates of particle P at any moment in a given coordinate system, and the known conditions are the initial coordinates and the initial movement trend.

To define the mathematical model of the motion modules, as shown in Figure 3, assume the particle P is on the initial position A, where the coordinates are (x_{st}, y_{st}, z_{st}), and in the first phase, the relationship between velocity and time is $V_1(t)$. After a certain time (t_1) of the movement, when the first phase is completed, the particle P moves to

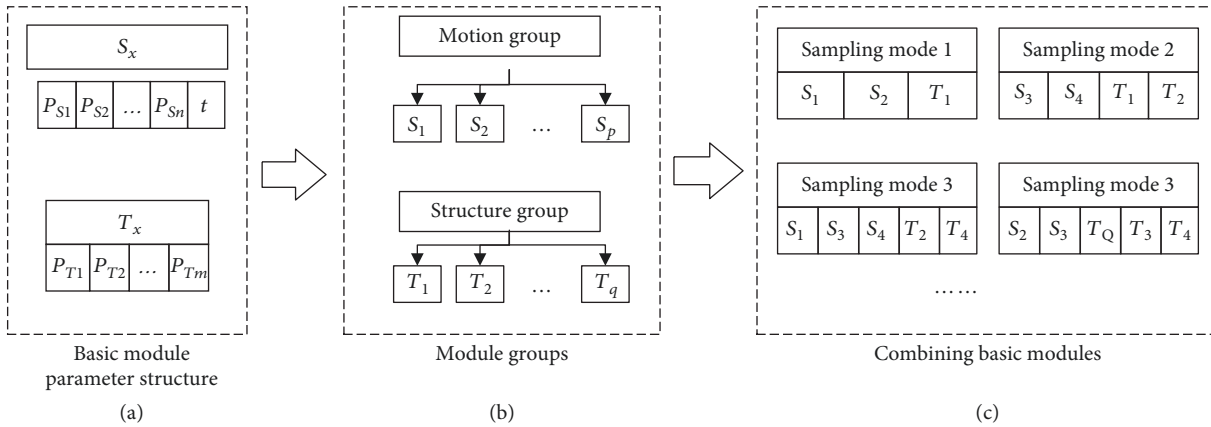

Figure 2: Modular motion-structure design model.

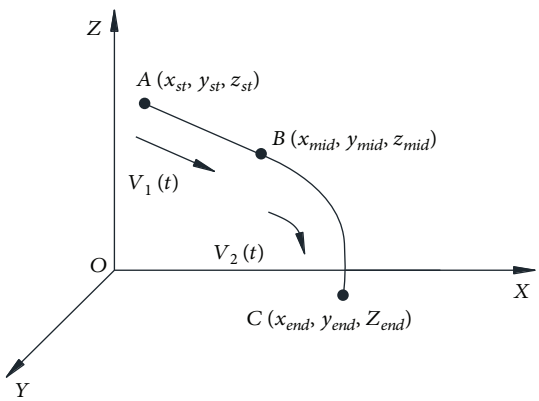

Figure 3: Motion module coordinate system.

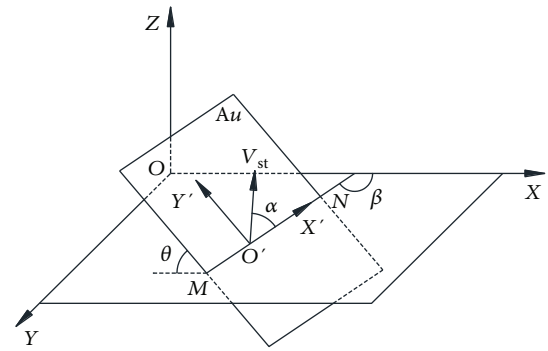

Figure 4: Auxiliary coordinate system for the motion module.

the position $B(x_{\text{mid}}, y_{\text{mid}}, z_{\text{mid}})$ and starts the second phase. In the second phase, which will last for an extended time (t_2), the relationship between velocity and time is $V_2(t)$, and the particle P will reach position $C(x_{\text{end}}, y_{\text{end}}, z_{\text{end}})$. During the period of $t_1 + t_2$, the trajectory of particle P, which is shown as the thick solid line in Figure 3, is described by the mathematical model defined as equation (1). In this formula, the coordinates (x, y, z) of particle P at any time are the dependent variables, and the independent variables are the initial coordinates $(x_{\text{st}}, y_{\text{st}}, z_{\text{st}})$, the movement trend $V_1(t), V_2(t)$, and time t. Equation (1) is the basic frame of the motion modules:

$$(x, y, z) = \begin{cases} S1(P_{\text{st}}, V_1(t), t), & t \in [0, t_1], \\ S2(P_{\text{mid}}, V_2(t), t), & t \in (t_1, t_2], \end{cases} \quad (1)$$

where P_{st} is the initial coordinate of particle P in the first phase that corresponds to the coordinates of position $A(x_{\text{st}}, y_{\text{st}}, z_{\text{st}})$ and P_{mid} is the initial coordinate of particle P in the second phase that corresponds to the coordinates of position $B(x_{\text{mid}}, y_{\text{mid}}, z_{\text{mid}})$, $P_{\text{mid}} = (x_{\text{mid}}, y_{\text{mid}}, z_{\text{mid}}) = S1(P_{\text{st}}, V_1(t_1), t_1)$.

2.2. Basic Modules in the Motion Group. From the perspective of speed, any motion with different accelerations can be divided into multiple ephemeral uniform motions. Regarding the trajectory, any tridimensional trajectory may be considered as the superposition of several rectilinear and circular trajectories. Hence, all tridimensional motions can be regarded as the combination of several tridimensional uniform rectilinear motions and circular motions, which can be defined as the basic modules for the motion group.

2.2.1. Auxiliary Coordinate System for Motion Modules. To establish the trajectory equation of tridimensional uniform rectilinear motion and circular motion, an auxiliary coordinate system is required, as shown in Figure 4. The auxiliary coordinate system is based on the global coordinate system XYZ shown in Figure 3, where the plane XOY is defined as the planetary surface. Assume the initial instantaneous velocity of sampling equipment is V_{st}, which is in the plane Au, and the initial position is O'. The angle between plane Au and plane XOY is $\theta(\theta \in [0, 90])$, and the intersecting line is MN (assuming the initial position O' is located on the intersecting line MN; i.e., all the sampling movements should start from the planetary surface, and the sampling initial position is the intersection position of the sampling equipment and the planetary surface). The angle $\beta(\beta \in [0, 360])$ is defined as the angle between the intersecting line MN and axis X, and its positive direction is counterclockwise from the positive axis X. Thus, an auxiliary coordinate system $X'O'Y'$ is established on the plane Au, where the axis

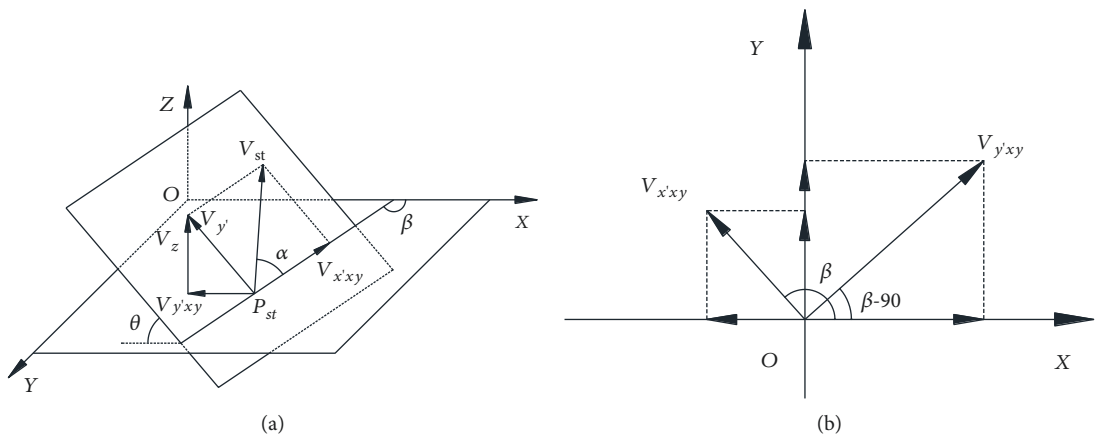

Figure 5: Decomposition of the three-dimensional velocity vector.

X' is the intersecting line MN and axis Y' is perpendicular to X'. Finally, define the angle $\alpha(\alpha \in [0, 360])$, which is the angle between initial velocity V_{st} and axis X'; its positive direction is counterclockwise from the positive axis X'.

2.2.2. Basic Module of Tridimensional Uniform Rectilinear Motion. In a three-dimensional space, the decomposition of the initial velocity vector is the core of uniform rectilinear motion trajectory analysis. Assuming the initial position is $P_{st}(x_{st}, y_{st}, z_{st})$, the velocity is V_{st} and this movement will cost time t. According to the basic equation of uniform rectilinear motion, the end position $P_{end}(x_{end}, y_{end}, z_{end})$ can be calculated as follows:

$$P_{end} = P_{st} + V_{st}t. \tag{2}$$

Bringing the initial velocity V_{st} into the auxiliary coordinate system $X'O'Y'$, as shown in Figure 5(a), the velocity vector V_{st} can first be decomposed into vector $V_x{}'xy$ and vector $V_{y'}$, as in equation (3). The vector $V_{x'xy}$ is parallel to axis X' and in the plane XOY, and the vector $V_{y'}$ is parallel to axis Y'.

$$\begin{aligned} &\overrightarrow{V_{st}} = \overrightarrow{V_{x'xy}} + \overrightarrow{V_{y'}}, \\ &\begin{cases} V_{x'xy} = V_{st}\cos\alpha, \\ V_{y'} = V_{st}\sin\alpha. \end{cases} \end{aligned} \tag{3}$$

Second, decompose the vector $V_{y'}$ into vector $V_y{}'xy$ and vector V_z, where vector $V_y{}'xy$ is perpendicular to axis X' and in the plane XOY and vector V_z is straight up:

$$\begin{aligned} &\overrightarrow{V_{y'}} = \overrightarrow{V_{y'xy}} + \overrightarrow{V_z}, \\ &\begin{cases} V_{y'xy} = V_{y'}\cos\theta, \\ V_z = V_{y'}\sin\theta. \end{cases} \end{aligned} \tag{4}$$

The vectors $V_x{}'xy$ and $V_y{}'xy$ are all in the plane XOY, and after transformation, the two vectors become the vector V_x and V_y, as shown in Figure 5(b):

$$\begin{aligned} &\overrightarrow{V_x} + \overrightarrow{V_y} = \overrightarrow{V_{x'xy}} + \overrightarrow{V_{y'xy}}, \\ &\begin{cases} V_x = V_{x'xy}\cos\beta + V_{y'xy}\cos(\beta - 90) = V_{x'xy}\cos\beta + V_{y'xy}\sin\beta, \\ V_y = V_{x'xy}\sin\beta + V_{y'xy}\sin(\beta - 90) = V_{x'xy}\sin\beta - V_{y'xy}\cos\beta. \end{cases} \end{aligned} \tag{5}$$

From equation (3) to equation (5), in three-dimensional coordinate system XYZ, the initial velocity vector V_{st} can be decomposed as three basic vectors along the corresponding axis $X/Y/Z$ as follows:

$$\begin{aligned} &\overrightarrow{V_{st}} = \overrightarrow{V_x} + \overrightarrow{V_y} + \overrightarrow{V_z}, \\ &\begin{cases} V_x = V_{st}(\cos\alpha\cos\beta + \sin\alpha\sin\beta\cos\theta), \\ V_y = V_{st}(\cos\alpha\sin\beta - \sin\alpha\cos\beta\cos\theta), \\ V_z = V_{st}\sin\alpha\sin\theta. \end{cases} \end{aligned} \tag{6}$$

According to equation (6) and equation (2), the basic mathematical module S_{line} of tridimensional uniform rectilinear motion is given by

$$\begin{aligned} &(x_{end}, y_{end}, z_{end}) = S_{line}((x_{st}, y_{st}, z_{st}), V_{st}, \alpha, \beta, \theta, t), \\ &\begin{cases} x_{end} = x_{st} + V_{st}t(\cos\alpha\cos\beta + \sin\alpha\sin\beta\cos\theta), \\ y_{end} = y_{st} + V_{st}t(\cos\alpha\sin\beta - \sin\alpha\cos\beta\cos\theta), \\ z_{end} = z_{st} + V_{st}t\sin\alpha\sin\theta. \end{cases} \end{aligned} \tag{7}$$

2.2.3. Basic Module of Tridimensional Uniform Circular Motion. Assume that there is a random particle P performing a tridimensional uniform circular movement, for which the radius is R, the initial position is $P_{st}(x_{st}, y_{st}, z_{st})$, and the initial linear speed is V_{st}. After a period of time t, particle P reaches the end position $P_{end}(x_{end}, y_{end}, z_{end})$. The solid

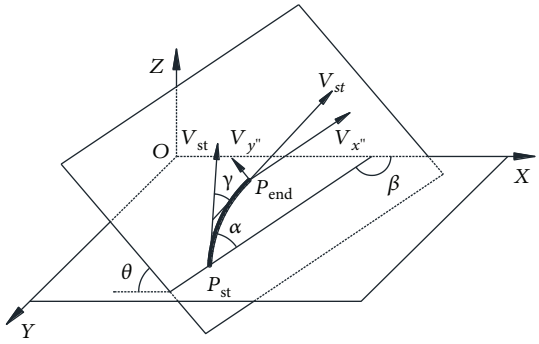

Figure 6: Analysis of uniform circular motion in three dimensions.

line of Figure 6 presents the trajectory for particle P, and the angular velocity ω_{st} can be calculated as

$$\omega_{st} = V_{st}/R. \tag{8}$$

According to equation (8), when particle P reaches its end position, the deflection angle γ of initial linear velocity V_{st} is given by equation (9), and the positive direction of γ is counterclockwise from the positive axis X'

$$\gamma = \omega_{st} t. \tag{9}$$

Over the entire movement period, the value of initial linear vector V_{st} remains the same, while the direction changes. At the end position, decomposing the velocity V_{st} into velocity vector $V_{x''}$ parallel to axis X' and vector $V_{y''}$ parallel to axis Y' in the auxiliary coordinate system $X'O'Y'$, we have

$$\begin{aligned} &\overrightarrow{V_{st}} = \overrightarrow{V_{x''}} + \overrightarrow{V_{y''}}, \\ &\begin{cases} V_{x''} = V_{st} \cos(\alpha - \gamma), \\ V_{y''} = V_{st} \sin(\alpha - \gamma). \end{cases} \end{aligned} \tag{10}$$

If the circumference can be seen as consisting of multiple very short segments, assuming at the moment of time t, particle P maintains the same velocity (both value and direction) and continues to move in a very short time dt. At the end of period of dt, the displacement of the particle P is given by

$$\begin{cases} X'' = V_{x''} dt, \\ Y'' = V_{y''} dt. \end{cases} \tag{11}$$

Combining equation (8) to equation (11) and evaluating the entire period of time t, the total displacement in both directions of X' and Y' can be calculated as equation (12), in which the symbol ± represents the change of the motion direction.

$$\begin{cases} X' = \int_0^t X'' = \int_0^t V_{st} \cos(\alpha \pm V_{st} t/R) dt = R(\mp \sin\alpha \pm \sin(\alpha \pm V_{st} t/R)), \\ Y' = \int_0^t Y'' = \int_0^t V_{st} \sin(\alpha \pm V_{st} t/R) dt = R(\pm \cos\alpha \mp \cos(\alpha \pm V_{st} t/R)). \end{cases} \tag{12}$$

According to equation (12), the end position $P_{end}(X', Y')$, which is in the auxiliary coordinate system $X'O'Y'$, can be calculated. Moreover, through the mapping relationship between auxiliary coordinate system $X'O'Y'$ and initial coordinate system XYZ, the coordinates $(x_{end}, y_{end}, z_{end})$ of the same position P_{end} can also be calculated. From equation (3) to equation (5), this mapping relationship is given as follows:

$$\begin{cases} x_t = x_t' \cos\beta + y_t' \sin\beta \cos\theta, \\ y_t = x_t' \sin\beta - y_t' \cos\beta \cos\theta, \\ z_t = y_t' \sin\theta. \end{cases} \tag{13}$$

Bringing the results from equation (12) into equation (13), the basic mathematical module S_{circle} for tridimensional uniform circular motion is given as

$$\begin{aligned} &(x_{end}, y_{end}, z_{end}) = S_{circle}((x_{st}, y_{st}, z_{st}), V_{st}, \alpha, \beta, \theta, t, R), \\ &\begin{cases} x_{end} = x_{st} + R[\mp\sin\alpha \cos\beta \pm \sin(\alpha \pm V_{st} t/R) \cos\beta \pm \cos\alpha \sin\beta \cos\theta \mp \cos(\alpha \pm V_{st} t/R) \sin\beta \cos\theta], \\ y_{end} = y_{st} + R[\mp\sin\alpha \sin\beta \pm \sin(\alpha \pm V_{st} t/R) \sin\beta \mp \cos\alpha \cos\beta \cos\theta \pm \cos(\alpha \pm V_{st} t/R) \cos\beta \cos\theta], \\ z_{end} = z_{st} + R[\pm\cos\alpha \sin\theta \mp \cos(\alpha \pm V_{st} t/R) \sin\theta]. \end{cases} \end{aligned} \tag{14}$$

2.3. Application of the Motion Group

2.3.1. Calculation Procedure of the Motion Group. The main function of the motion group is to calculate the trajectory of the sampling movement by freely combining the basic modules from two groups. The trajectory drawing process is as follows:

(1) Standardizing the parameters of the basic modules

To achieve the objective of freely combining modules, the two types of basic modules in the motion group should have the same types of input and output parameters. From the derivation of Section 2.2, the uniform rectilinear module S_{line} and the uniform circular module S_{circle} do have the same

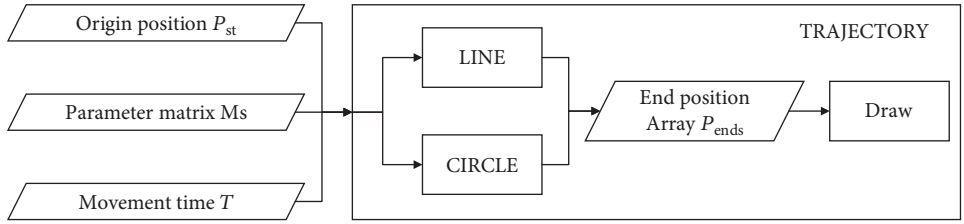

Figure 7: Program modules with internal logic.

output parameters $\text{output}_S = \{(x_{end}, y_{end}, z_{end})\}$. In terms of the input parameters, the parameter of the radius R is only in module S_{circle}. Hence, the radius R will be added into module S_{line} to ensure the unity of the input parameters. Theoretically, uniform rectilinear motion can be seen as a uniform circular motion with an infinite radius $R = \infty$. In the actual calculation, in module S_{line}, the radius can be set as $R = 0$, which indicates that the radius will not be involved in the calculation. More importantly, the parameter of radius R can be used to distinguish the rectilinear motion S_{line} and the circular motion S_{circle}. Thus, the same input parameters for both basic modules in the motion group can be obtained as $\text{Input}_S = \{(x_{st}, y_{st}, z_{st}), V_{st}, \alpha, \beta, \theta, t, R\}$.

(2) Creating the matrix of input parameters

To create the matrix of input parameters, first, division of the entire movement trajectory is necessary. The entire movement trajectory consists of several uniform rectilinear motions and circular motions, each of which will last different times, denoted as $t_1, t_2, t_3, \ldots, t_n$. Next, the input parameters are extracted from each motion; combined with the duration time, the entire matrix M_S is formed as given by

$$M_S = \begin{bmatrix} t_1 & R_1 & \alpha_1 & \beta_1 & \theta_1 & V_{st1} \\ t_2 & R_2 & \alpha_2 & \beta_2 & \theta_2 & V_{st2} \\ t_3 & R_3 & \alpha_3 & \beta_3 & \theta_3 & V_{st3} \\ \vdots & \vdots & \vdots & \vdots & \vdots & \vdots \\ t_n & R_n & \alpha_n & \beta_n & \theta_n & V_{stn} \end{bmatrix}. \quad (15)$$

Remarkably, the initial position for each motion is not involved in this matrix because in the whole calculation process, only the origin initial position (x_{st}, y_{st}, z_{st}) is required for the first motion. In the subsequent calculations, the initial position is the end position of the previous calculations, as shown in the following:

$$(x_{st\_n}, y_{st\_n}, z_{st\_n}) = (x_{end\_n-1}, y_{end\_n-1}, z_{end\_n-1}), \quad n \geq 1. \quad (16)$$

(3) Writing the related calculation program

To calculate movement trajectory, the program based on the basic motion group is comprised of four modules: the LINE module for calculating uniform rectilinear motion, the CIRCLE module for calculating uniform circle motion, the DRAW module for drawing trajectory, and the TRAJECTORY module for logic and data controlling. Figure 7 shows the internal logic relationships among the four modules. To control the whole process, the first step of the TRAJECTORY module is to receive the external parameters (including the original initial position P_{st}, the input parameter matrix M_S, and the entire movement time T). Next, the LINE module and the CIRCLE module are called in different periods according to the time division of parameter matrix M_S. Every calculation for both modules will calculate a temporary end position $P_{end1}, P_{end2}, P_{end3}, \ldots$. After completing all the calculations, all the temporary end positions can be integrated as an end position array P_{ends}. Finally, to complete the entire calculation, the DRAW module will be called to draw the entire trajectory by using the end position array P_{ends}. Figure 8 shows the detailed calculation process and the data flow of the whole program.

2.3.2. Example for Motion Group Application. Here, consider the example of the sampling movement of Phoenix Mars Lander, which landed on Mars on May 25th, 2008. To complete the sampling mission, a 2.35 m long Robotic Arm (RA) was used on the Phoenix Mars Lander; the RA had a 4-degree-of-freedom manipulator with a scoop at the top (Figure 9(a)). The scoop contained a front chamber and a rasp bit. The front chamber was designed to collect loose soil from the surface, and the rasp bit was designed for acquiring compact icy soil [15, 16].

The sampling process of the RA is shown in Figures 9(b)–9(d). Figure 9(b) shows that the direction of sampling movement moved toward the Phoenix Lander itself. According to Figure 9(c) (where the photo was taken on the Phoenix) and Figure 9(d) (which shows the sampling trace), the movement trajectory of the front chamber in the sampling process can be divided into five stages:

(1) Stage one. To reduce the resistance force from the surface soil, the chamber digs into the Martian surface at a small tilting angle. At this stage, the chamber is in a linear motion, and the digging will continue until the design sampling depth is reached

(2) Stage two. The chamber is in a circular motion, and its forward direction will change from a tilted to a horizontal position

(3) Stage three. The chamber continues to move along the horizontal direction and continues to collect the sample

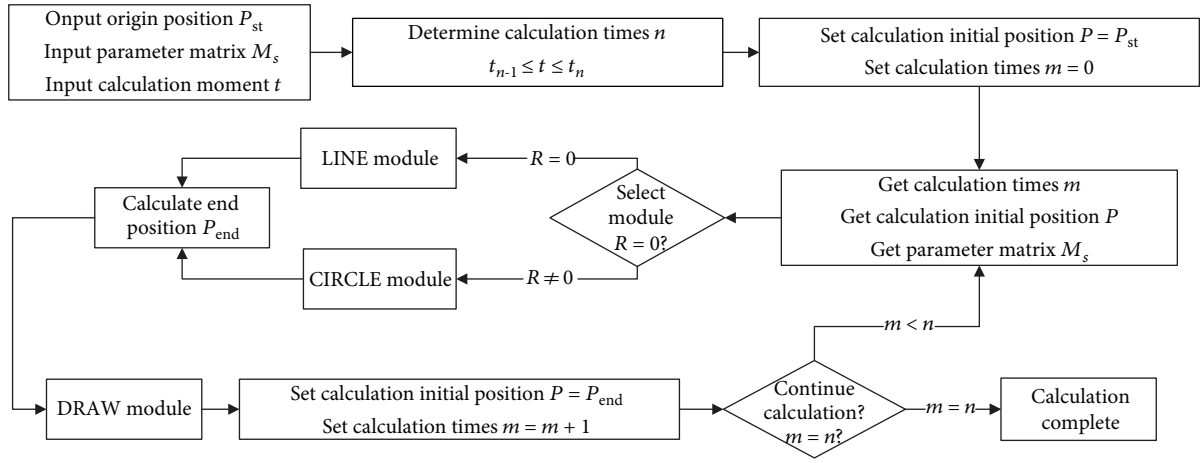

Figure 8: Calculation process and data flow in the program.

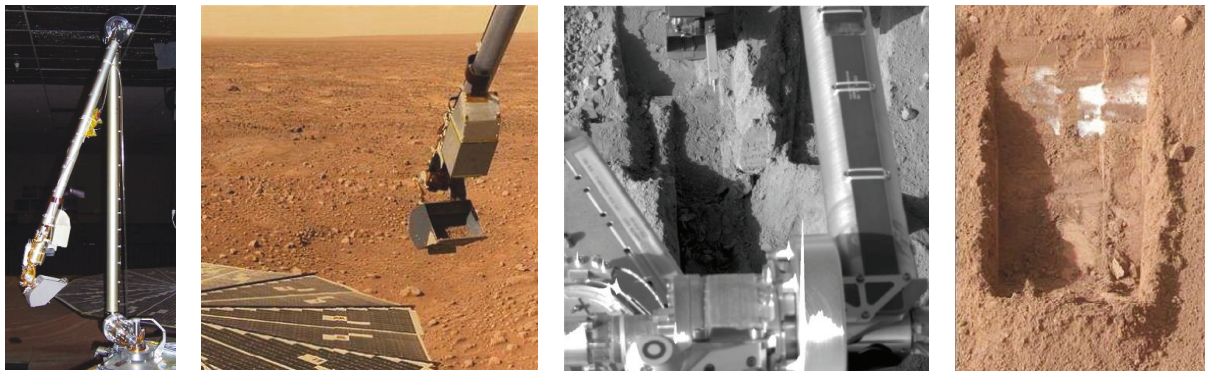

(a) (b) (c) (d)

Figure 9: Phoenix Mars Lander Robotic Arm and its sampling process.

(4) Stage four. Until enough soil is collected, the chamber begins to perform circular movement; i.e., the forward direction will be changed back to the tilted position. However, the tilting angle will be much larger than that in stage one to prevent loss of the sample

(5) Stage five. At the final stage, the chamber continues performing linear movements until it leaves the surface

In summary, the sampling trajectory for the digging chamber of the Phoenix Mars Lander can be defined as

$$S_P = \{S1_{\text{line}}, S2_{\text{circle}}, S3_{\text{line}}, S4_{\text{circle}}, S5_{\text{line}}\}. \quad (17)$$

Assume that particle A is on the blade edge of the front chamber. To establish an initial coordinate system XYZ, the Mars surface can be set to plane XOY, and the origin O is set to the initial position of particle A. Because the actual movement trajectory parameters are undocumented, the trajectory calculation here is based on the assuming parameters as follows. For the whole sampling process, assume that the linear speed of the chamber remains the same at 5 mm/s, and the distance between particle A and rotation axis is 100 mm. For stage one, the tilting angle, which is defined as the angle between the digging direction and the surface, is set to 30°, which is assumed to provide the maximum insertion force. For stage three, the sampling depth is set to 10 cm, and the maximum horizontal displacement of RA is set to 500 mm. For stage four, to prevent sampling loss during the lifting process, the minimum tilting angle for the front chamber is set to 75°.

According to the auxiliary coordinate system shown in Figure 4, to simplify the calculation, the plane Au can be set to a vertical plane parallel to plane XOZ. Hence, the positional parameters are $\beta = 0$ and $\theta = \pi/2$ (in the computer calculation, the angle values must be in radians); thus, the input parameter matrix M_{SP} for this assuming movement trajectory can be obtained, as given by the following:

$$M_{SP} = \begin{bmatrix} 34.64 & 0 & -\pi/6 & 0 & \pi/2 & 5 \\ 10.47 & 100 & -\pi/6 & 0 & \pi/2 & 5 \\ 39.30 & 0 & 0 & 0 & \pi/2 & 5 \\ 26.18 & 100 & 0 & 0 & \pi/2 & 5 \\ 5.36 & 0 & 5\pi/12 & 0 & \pi/2 & 5 \end{bmatrix}. \quad (18)$$

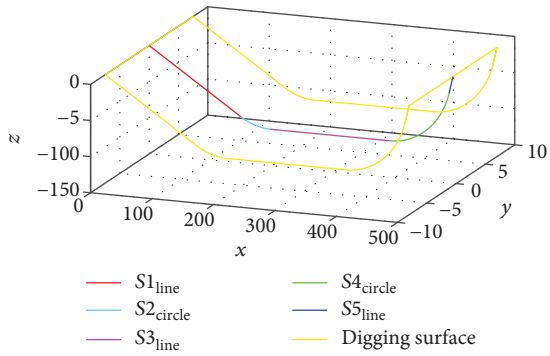

Figure 10: Movement trajectory calculation model.

Introducing the matrix M_{SP} into the program described in Figures 7 and 8, the assumed movement trajectory of particle A on the front chamber can be calculated, as shown by the solid line in Figure 10. If the width of the front chamber is 15 mm, then the trajectory of particle A can be moved to both sides by 7.5 cm to obtain the digging surface, as shown by the dashed line in Figure 10.

3. Structure Module Group

3.1. Structure Module Definition. The main target for the new design model is to analyse the interaction relationship between the sampling devices and the samples. According to this target, the structure modules discussed in this paper are focused on those structures that will contact with the sample and generate relative movement. For those structures that do not contact the sample, they hardly affect the analysis of interaction relationship and thus are not considered in the following discussion.

Through the investigation of the planetary sampling equipment in the introduction chapters, for deep sampling, the sampling structures around the world nearly have the same external shape, which is typically a spiral. In addition, the only distinction is in the specific parameter values, such as diameter, length, and helix angle. In terms of surface sampling, because of the different sampling requirements and space, there are obvious different structure designs shown in Figure 11. In addition, these obvious differences bring about significant difficulty on the analysis of interaction relationship. For example, when designing a piece of sampling equipment, traditionally, the structure that comes into contact with the sample is to be evaluated as a whole; i.e., the calculation, simulation, and experiments for this structure are disposable. If there is any microscopic modification or optimization of this structure, all of the studies must be repeated, leading to substantial waste of both research resources and time.

To solve this problem, establishing a relatively unified and flexible structure model is necessary, as this model can transform smoothly among different structures without repeating any of the research efforts for potential modification or optimization. Modular design for the sampling structure is the key to this solution. Essentially, every surface sampling structure can be viewed as consisting of multiple regular modules. Because of the regular external shapes, the calculation, simulation, or experiment works of these modules can easily achieve results with higher accuracy. More importantly, these results can be reused. For example, for a random sampling structure that consists of several modules, the analysis result of this structure can be achieved by combining the results of the analysis of the selected modules. When the structure must be modified, instead of repeating the calculation, simulation, and experiment works, the design work can be simplified to add or remove several ?modules via their analysis results. As shown in Figure 11, although the sampling devices are quite different around the world, each of them can be viewed as being composed of several flat plates or curved plates. Hence, the flat plate (curved plate) is selected as the basic module of the structure module group.

3.2. Basic Modules in the Structure Group. To meet the requirements of modular design and bring convenience to module combination, the structure modules should share a set of unified parameters. Traditionally, the parametric definition for any equipment is focused on its integral external structure. However, the parameter types (or numbers) are typically quite different among the various structures; as a result, this type of parametric definition cannot be used for the structure module. The parameters for structure modules here are defined according to their manufacturing processes:

(1) Section parameters. As shown in Figure 12(a), the cross section of the flat plate is rectangular and that for the curved plate can be considered as a bent rectangle. Therefore, the section parameters contain the rectangle length L_L, rectangle width L_W and bending radius R_L. The bending radius is $R_L = 0$ for flat plates. For curved plates, the rectangle length L_L denotes the length of the maximum arc, and the bending radius R_L is the radius of the maximum arc

(2) Extension parameters. After establishing the cross section, define the extension length L_E to enable it to extend toward the vertical direction

(3) Cutting parameters. Cutting will dramatically improve the flexibility and variability of the flat plate (curved plate). The cutting here is similar to the scan-removal operation in the tridimensional CAD software. As shown in Figure 12(c), the shaded areas will be cut and removed. First, the initial position of cutting is defined to be on the left edge of the upper surface along the extension direction, and the distance between the initial position and cross section is $L_C(L_C \in [0, L_E])$. Next, define the cutting contour on horizontal planes as well as the scan path on the vertical planes, and have the cutting contour perform "scan-removal" work along the scan path. According to the derivation in Section 2.2, any graphic is comprised of a segment and an arc, both of which can be fully defined by the initial speed, angle, and radius (the value of the radius for segments is equal to zero). For the cutting parameters, speed is completely unnecessary, whereas the angle and radius are required for both the cutting contour

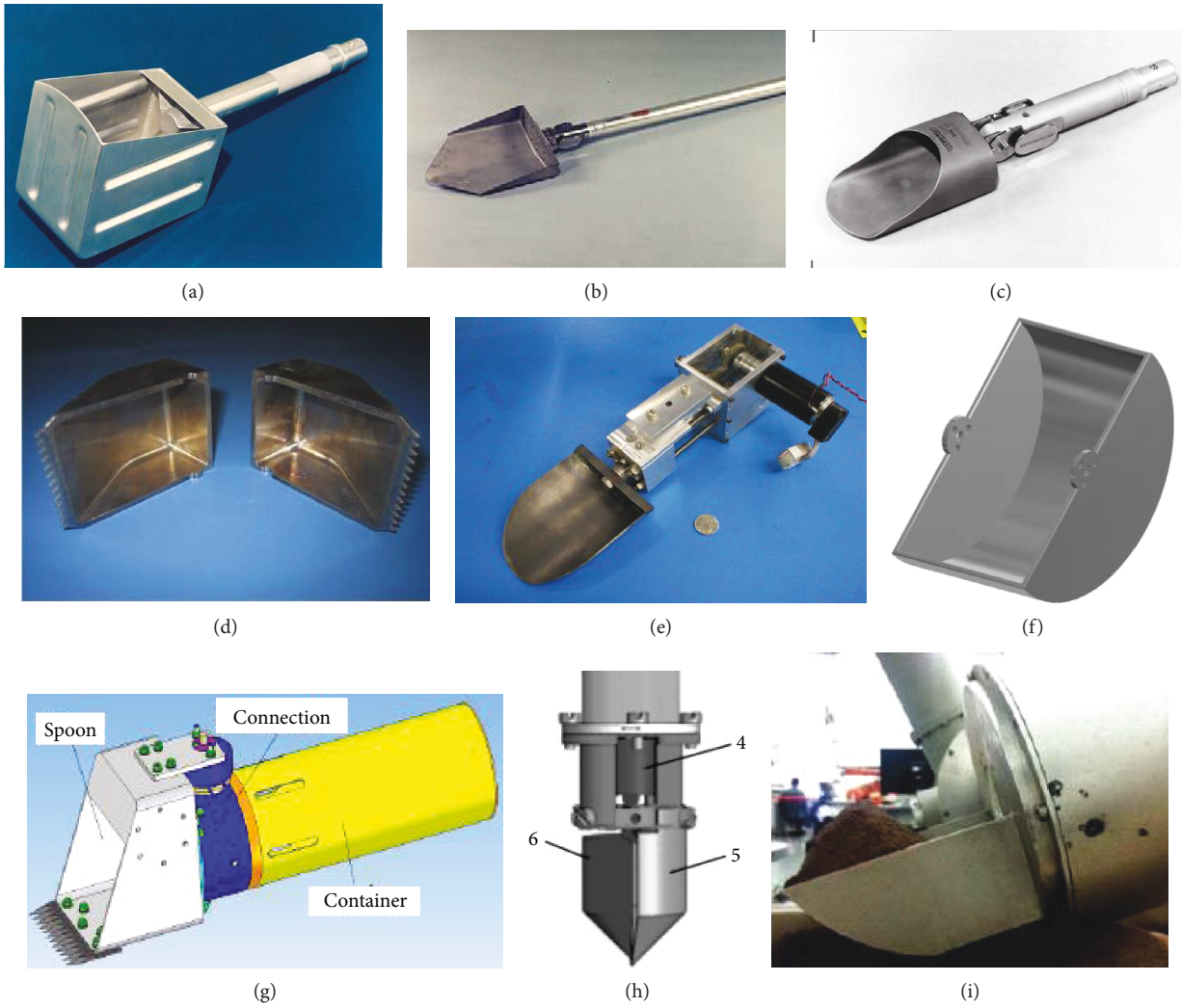

Figure 11: Planetary surface sampling devices around the world. (a–c) surface sampling equipment used in the Apollo Projects [17]; (d) SRR2k designed for the Mars 2018 project [18]; (e) digging equipment designed by Honeybee Corp. [19]; (f) sampling equipment designed by Keio University [20]; (g–i) surface sampling equipment designed for the Chinese lunar project [21–24].

and the scan path. The initial angle of the cutting contour is defined as γ_{HC}, where $\gamma_{HC} \in [0, 180]$, and its positive direction is clockwise from the extension direction of the cross section. In addition, the initial angle of the scan path is γ_{VC}, where $\gamma_{VC} \in [0, 180]$, and its positive direction is counterclockwise from the extension direction of cross section. Finally, the initial radius for the cutting contour and the scan path are defined as R_{HC} and R_{VC}

Thus, the mathematical definition for basic structure module T is

$$T = T(L_L, L_w, R_L, L_E, L_C, \gamma_{HC}, R_{HC}, \gamma_{VC}, R_{VC}). \tag{19}$$

According to the modular design theory, a sampling device consists of several basic modules; assuming the number is m, this sampling device can be defined by matrix M_T:

$$M_T = \begin{bmatrix} L_{L1} & L_{W1} & R_{L1} & L_{E1} & L_{C1} & \gamma_{HC1} & R_{HC1} & \gamma_{VC1} & R_{VC1} \\ L_{L2} & L_{W2} & R_{L2} & L_{E2} & L_{C2} & \gamma_{HC2} & R_{HC2} & \gamma_{VC2} & R_{VC2} \\ L_{L3} & L_{W3} & R_{L3} & L_{E3} & L_{C3} & \gamma_{HC3} & R_{HC3} & \gamma_{VC3} & R_{VC3} \\ \vdots & \vdots & \vdots & \vdots & \vdots & \vdots & \vdots & \vdots & \vdots \\ L_{Lm} & L_{Wm} & R_{Lm} & L_{Em} & L_{Cm} & \gamma_{HCm} & R_{HCm} & \gamma_{VCm} & R_{VCm} \end{bmatrix}. \tag{20}$$

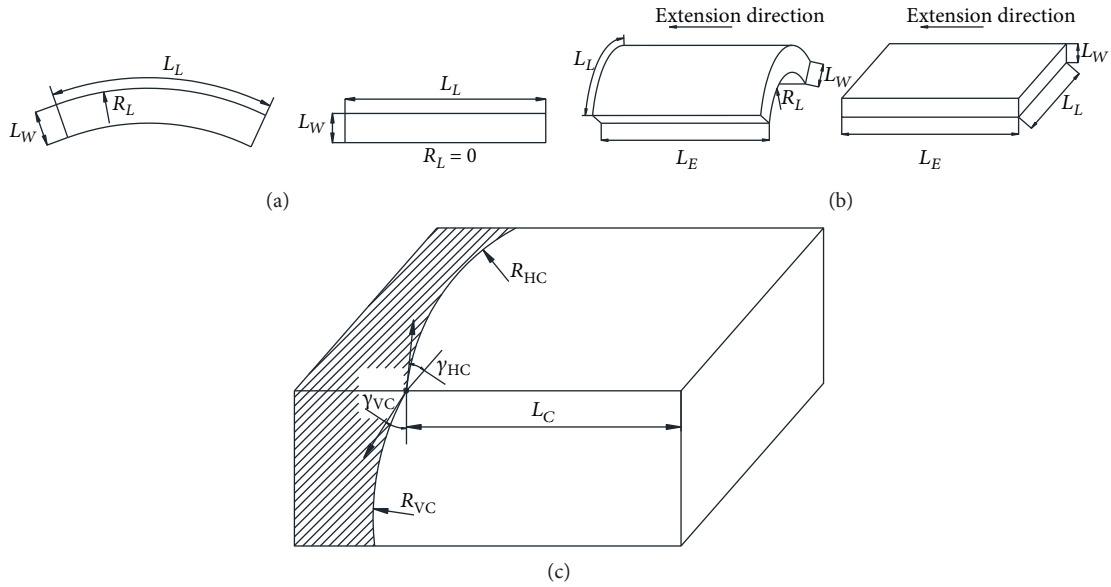

Figure 12: Definitions of the basic structure module.

3.3. Application of the Structure Group. Equation (19) defines the basic modules of the structure group by using a set of unified parameters, and equation (20) defines random surface sampling devices using a parameter matrix. For example, the digging spoon used in the Apollo Projects, as shown in Figure 11(c), can be decomposed into nine basic modules (Figure 13). In these modules, modules 1, 3, 5, 6, and 8 are flat plates and modules 2, 4, 7, and 9 are curved plates. The parameter definition of these basic modules is shown in Table 1.

Assuming that the thickness of the digging spoon is 5 mm, combined with the relative proportion of its structure, the assumed defining matrix M_T for the digging spoon is

$$M_T = \begin{bmatrix} T_1 \\ T_2 \\ T_3 \\ T_4 \\ T_5 \\ T_6{}^* \\ T_7 \\ T_8 \\ T_9 \end{bmatrix} = \begin{bmatrix} 120 & 5 & 0 & 250 & 229.6 & 52.5 & 98.5 & 90 & 0 \\ 62.8 & 5 & 20 & 217.4 & 192 & 32.1 & 0 & 90 & 0 \\ 40 & 5 & 0 & 192 & 128.2 & 32.1 & 0 & 90 & 0 \\ 62.8 & 5 & 20 & 128.2 & 95.9 & 32.1 & 0 & 90 & 0 \\ 120 & 5 & 0 & 103.9 & 103.9 & 135.4 & 84.5 & 32.1 & 0 \\ 40 & 5 & 0 & 80 & 60 & 90 & 20 & 90 & 0 \\ 62.8 & 5 & 20 & 128.2 & 128.2 & 122.1 & 0 & 90 & 0 \\ 40 & 5 & 0 & 192 & 192 & 122.1 & 0 & 90 & 0 \\ 62.8 & 5 & 20 & 217.4 & 217.4 & 122.1 & 0 & 90 & 0 \end{bmatrix}. \quad (21)$$

where $*$ means there are four identical modules T_6 with identical parameters; here, only one of them is listed.

4. Coupling Analysis between the Motion and Structure Groups

4.1. Principle of Coupling Analysis. Coupling analysis describes the connection between the motion and structure groups, and the coupling also plays an important role in achieving accurate research results. As shown in Figure 14(a), the entire sampling trajectory can be divided into several basic motion modules; similarly, the entire sampling equipment is composed of several basic structure modules. Hence, the whole sampling process transforms into two mathematical aggregations, and the coupling analysis can be simplified to study the connection between the basic motion module and the basic structure module.

As shown in Figures 14(b)–14(d), there are only three types of applications in the connection studies:

(1) Analysis of one structure module connected with all movement trajectories to obtain the force analysis

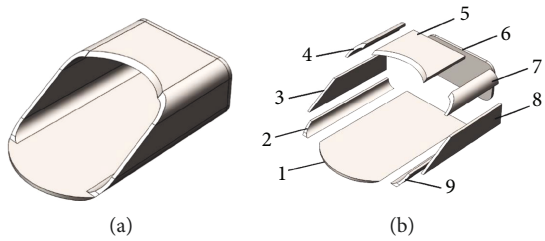

Figure 13: Disassembling schematic of the digging spoon used in the Apollo missions.

for one specific module in the whole sampling process (Figure 14(b))

(2) Analysis of all structure modules connected with one movement trajectory to obtain the force analysis of the entire sampling device in one specific sampling process (Figure 14(c))

(3) Analysis of all structure modules connected with all movement trajectories to obtain the force analysis of the entire sampling device in the whole sampling process (Figure 14(d))

The core of the connection research is to analyse the interaction relationship between the single motion module and the single structure module at any given moment. In the motion groups, tridimensional uniform rectilinear motion and tridimensional uniform circular motion are the basic modules. The major difference between the two modules is the velocity during the entire movement process. For rectilinear motion, both the initial value and direction remain the same, whereas for circular motion, only the initial value will not change, and its direction changes with time. Therefore, in the connection research, the primary function for basic motion modules is to calculate the instantaneous velocity value and direction at any given moment.

In the structure groups, the flat and curved plates are the two basic modules. To obtain the entire force distribution of a basic module in the sampling process, force analysis must be performed on every surface of this module, according to the contact relationship between the surfaces and samples. First, the velocity direction for each surface should be obtained through the calculation of the basic motion modules. Next, the velocity direction is split into two directions: parallel to the surface and perpendicular to the surface. According to the definition of the basic structure module, there are only two types of surfaces: flat and curved surfaces. Two types of velocity directions combined with two types of surfaces result in four different coupling analyses, as shown in Figure 15.

When the velocity direction is parallel to the surface (Figures 15(a) and 15(b)), the friction, which is the only force acting on the surface, is spread uniformly on the surface. When the velocity direction is perpendicular to the surface (Figures 15(c) and 15(d)), the only force acting on the surface is the reaction, which is also spread uniformly on the surface. The direction of both forces is opposite to the velocity direction. To calculate the resultant force for a flat surface, the calculation method is the surface area multiplied by the force per unit area. For a curved surface, the first step is to flatten it as a rectangular plane and then calculate the parameters as a flat surface.

By combining the force from every surface in every direction, the force analysis of a specific structure module at a given moment can be calculated. Similarly, the force analysis for a given sampling device can be calculated by combining the force from every structure module, which completes the connection study, i.e., the coupling analysis.

4.2. Examples of Coupling Analysis. Here, two examples are provided to briefly show the coupling analysis based on the motion and structure module groups. Assume that the digging spoon shown in Figure 13 is used to perform sampling; its movement trajectory is shown in Figure 10. Use the bottom structure module T_1 to perform coupling analysis in movement stage one $S1_{\text{line}}$ and stage two $S2_{\text{circle}}$.

4.2.1. Coupling Analysis for Structure Module T1 in Movement Stage $S1_{\text{line}}$. From equation (21), the parameter value of structure module T_1 is

$$T_1 = T(120, 5, 0, 250, 229.6, 52.5, 98.5, 90, 0). \quad (22)$$

Assume that the planetary surface is the plane $X = 0$, $Y = 0$, and the origin of coordinate system is the first point where the structure makes contact with the surface. The movement equation $S1_{\text{line}}$ of structure module T_1 in stage one can be obtained by using equation (18):

$$S1_{\text{line}} = S_{\text{line}}((0, 0, 0), 5, -\pi/6, 0, \pi/2, 34.64, 0). \quad (23)$$

As shown in Figure 16, the solid line represents the trajectory $S1_{\text{line}}$, and the structure module T_1 will perform a sampling movement along the trajectory. To enhance the display effect, in Figure 16, the thickness of structure module T_1 is increased; however, in actual calculation, the thickness should retain the origin value. Based on the principle of coupling analysis in Section 4.1, to analyse the entire force of structure module T_1, the primary task is to distinguish the contact areas because the contact generates forces and contact areas are varied among different surfaces. For structure module T_1, the bottom surface, upper surface, and left and right surfaces are parallel to the direction of velocity; therefore, the forces on these surfaces are friction, denoted as $F_{u1}, F_{d1}, F_{l1}, F_{r1}$, respectively. These frictional forces are caused by stress induced by depth and sample gravity in movement. Similarly, the front surface of structure module T_1 is a curved surface perpendicular to the velocity direction, which brings the reaction F_{t1} from the sample cutting resistance and bearing capacity corresponding to the movement. Hence, the total force for structure module T_1 in stage $S1_{\text{line}}$ is

$$F_{T1S1} = F_{u1} + F_{d1} + F_{l1} + F_{r1} + F_{t1}. \quad (24)$$

Table 1: Parameter definition of the digging spoon.

Module no.	Cross section	Cutting contour	Scan path	Zero value parameters	Lateral deflection
1	Flat	Arc	Segment	R_{L1}, R_{VC1}	
2, 9	Curved	Segment	Segment	$R_{\mathrm{HC2}}, R_{\mathrm{VC2}}$	90°
3, 8	Flat	Segment	Segment	$R_{L3}, R_{\mathrm{HC3}}, R_{\mathrm{VC3}}$	90°
4, 7	Curved	Segment	Segment	$R_{\mathrm{HC4}}, R_{\mathrm{VC4}}$	90°
5	Flat	Arc	Segment*	R_{L5}, R_{VC5}	
6**	Flat	Arc	Segment	R_{L6}, R_{VC6}	

*The scan path for module 5 is nonvertical; **the original shape for module 6 is a flat plate, where four corners should perform arc cutting, considering this plate is of symmetrical shape with two symmetrical axes; hence, the plate can be split into four identical plates along the vertical and horizontal axis.

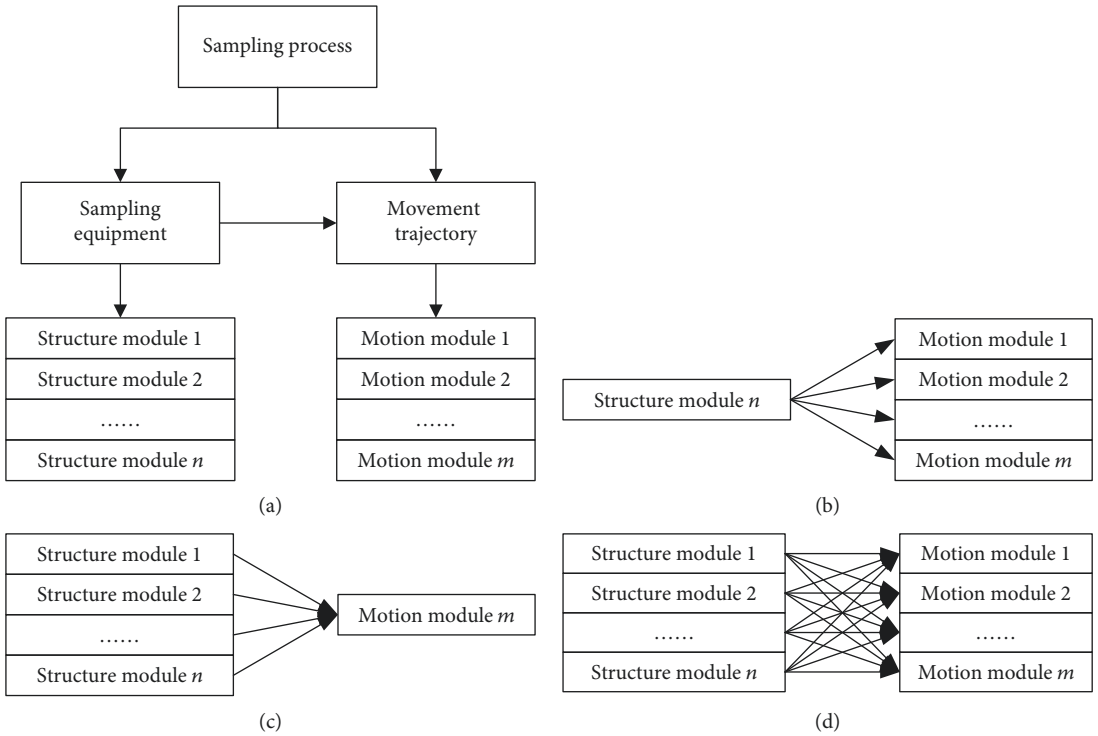

Figure 14: Principle of coupling analysis for the motion and structure groups.

4.2.2. Coupling Analysis for Structure Module $T1$ in Movement Stage $S2_{\mathrm{circle}}$. Assuming that the end position of stage $S1_{\mathrm{line}}$ is Pt_1, the movement equation of structure module T_1 in stage $S2_{\mathrm{circle}}$ is given by the following:

$$S2_{\mathrm{circle}} = S_{\mathrm{circle}}(Pt_1, 5, -\pi/6, 0, \pi/2, 10.47, 100). \quad (25)$$

When structure module T_1 performs a sampling work in stage $S2_{\mathrm{circle}}$, the trajectory is an arc (solid line in Figure 17). During the whole stage, the velocity direction is neither parallel nor perpendicular to the midaxis of structure module T_1 at any moment. Therefore, in the force analysis, the velocity v must be split into the component velocity v_h parallel to the midaxis and the component velocity v_v perpendicular to the midaxis.

Under the influence of velocity v_h, similar to stage $S1_{\mathrm{line}}$, the friction is spread uniformly on the bottom surface, upper surface, and left and right surfaces, represented as F_{u2h}, F_{d2h}, F_{l2h}, and F_{r2h} respectively. The reaction F_{t2h} is perpendicular to the front surface of structure module T_1.

Under the influence of velocity v_v, the friction, denoted as F_{l2v}, F_{r2v}, F_{t2v}, is spread throughout the front surface, left surface, and right surface. These frictional forces also originate from the stress caused by the depth and sample gravity during movement. For the upper surface, there is the reaction F_{u2v} induced by sample gravity. For the bottom surface, no force will be acting on it because this surface will detach from the sample.

Hence, the total force for structure module T_1 in stage $S2_{\mathrm{circle}}$ is

$$\begin{cases} F_{T1S2\_h} = F_{u2h} + F_{d2h} + F_{l2h} + F_{r2h} + F_{t2h}, \\ F_{T1S2\_v} = F_{u2v} + F_{l2v} + F_{r2v} + F_{t2v}. \end{cases} \quad (26)$$

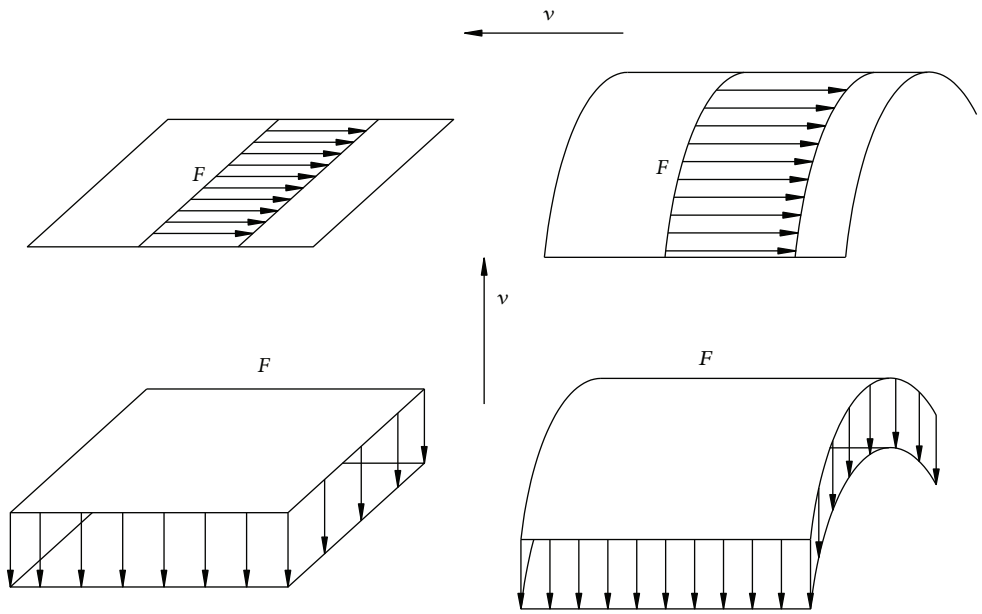

Figure 15: Coupling force analysis between the velocity and the surfaces.

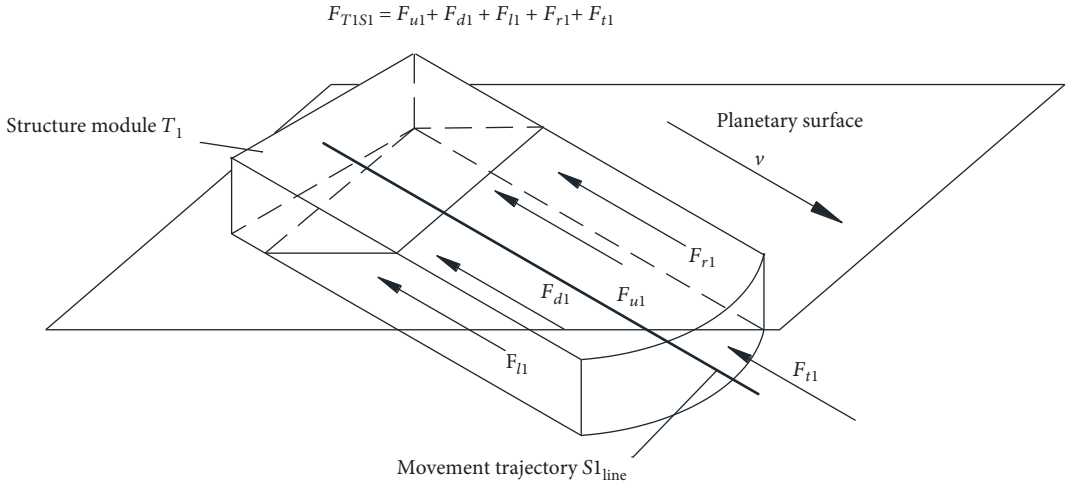

Figure 16: Force analysis for structure module T_1 in stage $S1_{line}$.

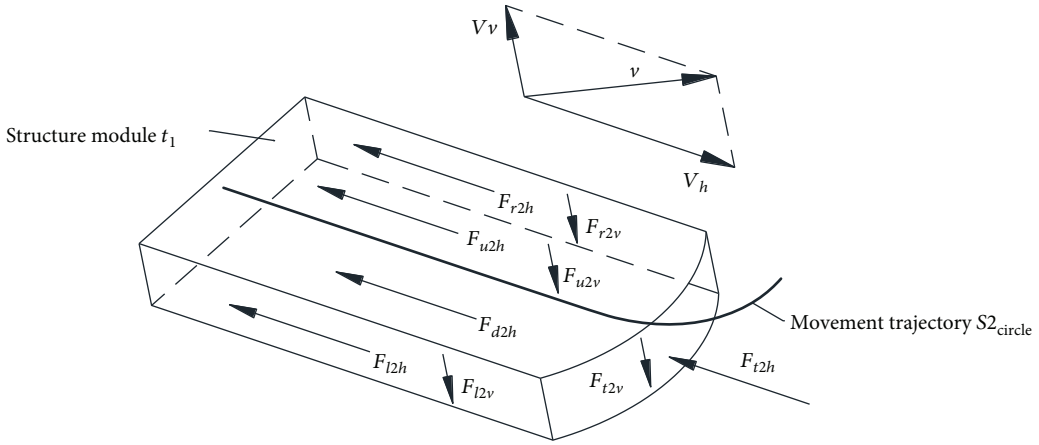

Figure 17: The force analysis for structure module T_1 in stage $S2_{circle}$.

5. Conclusion

A new modular motion-structure design model for surface sampling that freely combines the basic modules from the motion and structure groups was discussed in this paper. This model can be applied to different movements and equipment structures for more accurate definition and analysis results as follows:

(1) The main function of the motion group is to analyse the sampling movement trajectory and to obtain the required coordinates at any given moment during the sampling process. There are two basic modules in this group: tridimensional uniform rectilinear motion and tridimensional uniform circular motion. With the same input and output parameters, the two types of basic motion modules can be used to compose any sampling trajectory, as needed

(2) To adapt to the various external structures of the surface sampling equipment, the flat plate and the curved plate are selected as the basic modules in the structure group. Sharing the same parameters (including section, extension, and cutting parameters), the two types of basic modules can change their external shape by adjusting their parameters. More importantly, the same parameters make it convenient to combine different structure basic modules to define a complex sampling structure

(3) Based on the motion group and the structure group, the research on the entire sampling process transforms into the research studies on the motion groups, the structure groups and the coupling analysis between the two groups. The different types of combinations among the motion modules and the structure modules will lead to different results from the coupling analysis. According to the characteristics of the two groups, the key to performing the coupling analysis is to determine the force on the flat or curved surface as well as the influence of the velocity direction

Data Availability

No data were used to support this study.

Disclosure

We would like to declare on behalf of my coauthors that the work described was original research that has not been published previously and not under consideration for publication elsewhere, in whole or in part.

Conflicts of Interest

No conflict of interest exits in the submission of this paper, and it is approved by all authors for publication.

Authors' Contributions

All the authors listed have approved the manuscript that is enclosed.

Acknowledgments

The National Natural Science Foundation of China, with its financial support of the project research on Simulated Lunar Surface Sampling Machine-Soil Coupling Mechanics Model (no. 11502034) is gratefully acknowledged. In addition, Chengdu University of Technology and Institute of Exploration Technology (CAGS) are acknowledged for their experimental and theoretical support.

References

[1] Z. Ouyang, "Scientific objectives of Chinese lunar exploration project and development strategy," *Advance in Earth Sciences*, vol. 19, no. 3, pp. 351–358, 2004.

[2] M. E. Anttila, *Concept Evaluation of Mars Drilling and Sampling Instrument[Dissertation]*, Helsinki University of Technology, Holland, 2005.

[3] C. Pitcher and Y. Gao, "First implementation of burrowing motions in dual-reciprocating drilling using an integrated actuation mechanism," *Advances in Space Research*, vol. 59, no. 5, pp. 1368–1380, 2017.

[4] C. Pitcher and Y. Gao, "Analysis of drill head designs for dual-reciprocating drilling technique in planetary regoliths," *Advances in Space Research*, vol. 56, no. 8, pp. 1765–1776, 2015.

[5] G. Bianciardi, J. D. Miller, P. A. Straat, and G. V. Levin, "Complexity analysis of the Viking labeled release experiments," *International Journal of Aeronautical and Space Sciences*, vol. 13, no. 1, pp. 14–26, 2012.

[6] H. A. Judith, "Catalog of Apollo lunar surface geological sampling tools and containers," July 2016, http://www.hq.nasa.gov/alsj/tools/Welcome.html.

[7] "Chronology of Mars exploration," July 2016, http://nssdc.gsfc.nasa.gov/planetary/chronology_mars.html.

[8] V. Badescu and K. Zacny, "Lunar drilling, excavation and mining in support of science, exploration, construction, and in situ resource utilization (ISRU)," in *Moon*, V. Badescu, Ed., pp. 235–265, Springer Berlin Heidelberg, 2012.

[9] X. Xiao, *Dynamic Modeling and Control of a Bicycle Robot[Dissertation]*, Beijing University of Posts and Telecommunications, Beijing, 2018.

[10] S. Šalinić, G. Bošković, and M. Nikolić, "Dynamic modelling of hydraulic excavator motion using Kane's equations," *Automation in Construction*, vol. 44, pp. 56–62, 2014.

[11] J. E. Hurtado, "Analytical dynamics of variable-mass systems," *Journal of Guidance, Control and Dynamics*, vol. 41, no. 3, pp. 701–709, 2018.

[12] K. Skonieczny, D. S. Wettergreen, and W. L. "Red" Whittaker, "Advantages of continuous excavation in lightweight planetary robotic operations," *International Journal of Robotics Research*, vol. 35, no. 9, pp. 1121–1139, 2016.

[13] L. Xue, B. Chen, Z. Zhao, Z. Dang, and M. Zou, "Experimental study of torque using a small scoop on the lunar surface," *International Journal of Aerospace Engineering*, vol. 2016, Article ID 8035456, 8 pages, 2016.

[14] A. Green and K. Zacny, "Effect of Mars atmospheric pressure on percussive excavation forces," *Journal of Terramechanics*, vol. 51, pp. 43–52, 2014.

[15] R. Bonitz, L. Shiraishi, M. Robinson et al., "The Phoenix Mars Lander Robotic Arm," in *2009 IEEE Aerospace conference*, pp. 1–12, Big Sky, MT, USA, March 2009.

[16] "Phoenix (spacecraft)," July 2016, https://en.wikipedia.org/wiki/Phoenix_(spacecraft).

[17] J. H. Allton, *Lunar Samples: Apollo Collection Tools, Curation Handling, Surveyor III and Soviet Luna Samples*, Mcszulu, 2009.

[18] P. Younse, A. Stroupe, T. Huntsberger et al., "Sample acquisition and caching using detachable scoops for mars sample return," in *2009 IEEE Aerospace conference*, Big Sky, MT, USA, March 2009.

[19] J. Craft, J. Wilson, P. Chu, K. Zacny, and K. Davis, "Percussive digging systems for robotic exploration and excavation of planetary and lunar regolith," in *2009 IEEE Aerospace conference*, pp. 7–14, Big Sky, MT, USA, March 2009.

[20] D. Mori and G. Ishigami, "Excavation model of soil sampling device based on particle image velocimetry," *Journal of Terramechanics*, vol. 62, pp. 19–29, 2015.

[21] W. Lu, A. G. Song, and Y. Ling, "Research on sampler for shallow lunar regolith," *Journal of Astronautics*, vol. 9, pp. 2065–2073, 2011.

[22] S. Yang, L. G. Dong, S. Yin, J. Sun, G. X. Wang, and D. Zhang, "Research of lunar soil sampling devices based on swing arm with guide rail," *The Ninth Annual Symposium of Professional Committee of Chinese Society of Astronautics Deep Space Exploration Technology*, 2012, Hangzhou, China, 2012.

[23] C. Li, Z. Xie, Y. Li, and H. Liu, "A novel end-effector for lunar sample acquisition and return," *Robot*, vol. 35, no. 1, pp. 9–16, 2013.

[24] Y. S. Li, *Research on Surface Sampler of Lunar Exploration[Dissertation]*, Harbin Institute of Technology, Harbin, 2012.